Published in "Nature doi:10.1038/nature11001, 2012"
which should be cited to refer to this work.

Methods

PILS gene accession codes

Sequence data from this article can be found in The Arabidopsis Information Resource (TAIR; http://www.arabidopsis.org/) or GenBank/EMBL databases under the following accession numbers: PILS1 (At1g20925), PILS2 (At1g71090), PILS3 (At1g76520), PILS4 (At1g76530), PILS5 (At2g17500), PILS6 (At5g01990), PILS7 (At5g65980).

Plant material, growth conditions and DNA constructs

We used Arabidopsis thaliana of ecotype Columbia 0 (Col-0). The Nicotiana tabacum L. cv. Bright Yellow 2 (BY-2) cell line19 was used as suspension-cultured cells. pils2-1 (SALK_024808), pils2-2 (SALK_125391), pils5-1 (SALK_070653) and pils5-2 (SALK_072996) were obtained from the Nottingham Arabidopsis Stock Centre (NASC). Insertion sites were verified, homozygous lines selected and the decrease or absence of the respective PILS transcript was shown by RT–PCR. The pils2-2 and the pils5-2 mutants were crossed into DR5rev::GFP2. Gateway cloning was used to construct pPILS2::GFP::GUS, pPILS5::GFP::GUS, p35S::PILS1–7, p35S::GFP::PILS1–7, p35S::PILS1–7::GFP, pPILS5::PILS5::GFP and pMDC7_B(pUBQ)::PILS2. The PILS full-length genomic fragments, complementary DNA and promoter regions were amplified by PCR from genomic DNA and cDNA, respectively. The PCR was performed using the high fidelity DNA polymerase “I proof” (Bio-Rad). The primers used are given below. The full genomic and cDNA fragments were cloned into the pDONR221 (Invitrogen) vector and the promoter regions into pDONR-P4P1 using Invitrogen BP-clonase according to manufacturer’s instructions. Coding sequences were transferred from the entry clones to gateway-compatible destination vectors (given below) using the Invitrogen LR clonase(+) according to manufacturer’s instructions. The resulting constructs were transformed into Col-0 plants by floral dipping in Agrobacterium tumefaciens liquid cultures. Yeast vectors were transformed into budding yeast (Saccharomyces cerevisiae) via electroporation. The p35S::PILS5::GFP line was crossed into pDR5rev::mRFP1er20. The following lines and constructs have been previously described: pDR5rev::mRFP1er20, pDR5rev::GFP2 and p35S::GFP::HDEL21. Seeds were stratified at 4 °C for 2 days in the dark. Seedlings were grown vertically on half Murashige and Skoog medium. Plants were grown under long-day (16 h light/8 h dark) conditions at 20–22 °C.

Chemicals

1-Naphthaleneacetic acid (NAA) was supplied by Duchefa, 2,4-dichlorophenoxy acetic acid, oestradiol and propidium iodide by Sigma-Aldrich and 3H-indole-3-acetic acid (3H-IAA), 3H-naphthalene-1-acetic acid (3H-NAA) and 14C-benzoic acid (14C-BA) (specific radioactivity 20 Ci mmol−1) by American Radiolabelled Chemicals.

RNA extraction and quantitative real time PCR (qPCR)

Whole RNA of seedlings was extracted using the RNeasy Mini Kit (Qiagen) in technical triplicates, the extracted RNA samples were treated with DNase (Ambion). qPCR analysis was performed using ICycler (Bio-Rad) with the Platinum SYBR Green qPCR Super-UDG kit (Invitrogen) following recommendations of the manufacturer. qPCR was carried out in 96-well optical reaction plates heated for 10 min to 95 °C to activate hot-start Taq DNA polymerase, followed by 40 cycles of denaturation for 60 s at 95 °C and annealing-extension for 60 s at 58 °C. Target quantifications were performed with specific primer pairs (given later) designed using Beacon Designer 4.0 (Premier Biosoft International). Expression levels were normalized to the expression levels of translation initiation factor EIF4A. The primers used are given later.

Phenotype analysis

For analysis of the root length and lateral root density, plates were scanned on a flat-bed scanner. Root hairs were imaged with a binocular microscope (Leica). For hypocotyls analysis, seeds on plates were exposed to light for 3 h at 18 °C, and cultivated in the dark at 20 °C. Seedlings were imaged in real time with an infrared camera (Canon) to define the exact moment of germination and analysed 1, 3 and 5 days after germination. Hypocotyls, root and root hair lengths were measured with the ImageJ (http://rsb.info.nih.gov/ij/) software. Lateral root density for each seedling was obtained by calculating the number of lateral roots per root length unit 14 days after germination. For analysis of hypocotyls length, a minimum of 15 hypocotyls per condition or mutant line were analysed in each experiment. For analysis of root length and lateral root density, a minimum of 40 plants per condition or mutant line were analysed in each experiment. Means and standard errors were calculated and the statistical significance was evaluated by the student t-test using the GraphPad Prism5 (http://www.graphpad.com) software. For the analysis of root hair growth, 20 seedlings per transgenic line were imaged by binocular (Leica) and 20 root hairs (randomly chosen in the root hair zone) per seedling were measured with the ImageJ (http://rsb.info.nih.gov/ij/) software. The mean and standard error of the mean per transgenic line were calculated and the statistical significance was evaluated by the student t-test. To obtain the auxin-dependent root hair elongation, the same number of root hairs per seedling, seedlings per mutant line and condition were analysed as described above. The untreated mean average root hair length of the respective genotype was subtracted from the individual auxin-treated root hair length to obtain auxin induced growth in millimetre. The mean and standard error of the mean of the respective genotype were calculated and the statistical significance was evaluated by the student t-test using the GraphPad Prism5 (http://www.graphpad.com) software. All experiments were performed in at least three independent biological repetitions.

BY-2 plant material

Cells of tobacco line BY-2 (Nicotiana tabacum L., cv. Bright Yellow 2)19 transformed with pMDC7_B(pUBQ)::PILS2 were cultured in liquid cultivation medium (3% (w/v) sucrose, 4.3 g l−1 Murashige and Skoog salts, 100 mg l−1 inositol, 1 mg l−1 thiamine, 0.2 mg l−1 2,4-dichlorophenoxy

acetic acid, and 200 mg l−1 KH2PO4 (pH 5.8). BY-2 cell lines were cultivated in darkness at 26 °C on an orbital incubator (Sanyo Gallenkamp, Schöeller Instruments; 150 r.p.m., 32-mm orbit) and subcultured weekly. Stock BY-2 calli were maintained on media solidified with 0.6% (w/v) agar and subcultured monthly.

Transient transformation of BY-2 cells and monitoring of cellular auxin signalling in BY2

Ten ml of three-day-old cells were harvested on filter paper by vacuum filtration and kept on plates with solid BY-2 medium. The cells were transformed via particle bombardment with a PDS 1000/He biolistic system (Bio-Rad) according to the manufacturer's instructions (http://www.bio-rad.com/webroot/web/pdf/lsr/literature/Bulletin_9075.pdf). 2 µl of plasmid DNA (0.05 µg µl of the pDR5rev::mRFP1er contruct and 0.1 µg µl−1 of p35S::PILS2 and p35S::PILS5) was added to 6.25 µl of 1.6-µm diameter gold particles (dissolved in 50% glycerol). The suspension was supplemented with 2.5 µl spermidine (0.1 M stock solution) and 6.25 µl CaCl2 (2.5 M stock solution). The particles were pelleted by centrifugation, washed twice with 70% and 100% ethanol and, subsequently, resuspended in 10 µl of 100% ethanol. Cells were bombarded under a pressure of 1,100 pounds per square inch. The plates were sealed with Parafilm and kept in the dark for 18 h at 25 °C. For microscopic analysis, cells were gently transferred from the filter to a microscopy slide (in water) and subsequently covered with a cover slip. Samples were analysed via confocal microscopy. The pDR5rev::mRFP1er expression was evaluated by defining the mean grey value (MGV) of each imaged cell (middle sections). For each experiment, confocal settings were defined based on the pDR5rev::mRFP1er signal of the control cells and remained unchanged during the respective experiments. Transformants were identified on the basis of the fluorescence of both proteins and imaged with a ×40 objective. Every experiment/transformation was done in triplicate and for each condition a total number of at least 60 transformed cells were imaged. For each experiment, the means and standard errors were calculated and the statistical significance (independence between the two populations) was obtained by the student t-test using the GraphPad Prism5 (http://www.graphpad.com) software.

Immunocytochemistry

Whole-mount immunological staining on 5-day-old seedlings was done in an Intavis robot according to the described protocol22. The antibodies used at the final dilutions were monoclonal mouse anti-BIP2 (Hsc70) at 1:200 (Stressgen Bioreagents), monoclonal rabbit anti-GFP at 1:600 (Invitrogen). The secondary anti-mouse (Invitrogen) and anti-rabbit (Sigma-Aldrich) antibodies conjugated with Cy3 and Alexa488 respectively were used at 1:600 dilution.

Microscopy

Confocal microscopy was done with a Zeiss 710 microscope (Zeiss) or Leica SP5 (Leica). Fluorescence signals for GFP (excitation 488 nm, emission peak 509 nm), mRFP1 (excitation 561 nm, emission peak 607 nm) and propidium iodide (PI) staining (excitation 536 nm, emission peak 617 nm) were detected with a ×20, ×40 (water immersion) or ×63 (water immersion) objective. Sequential scanning was used

for double labelling to avoid crosstalk between channels. Fluorescence signal intensity was analysed with ImageJ (http://rsb.info.nih.gov/ij/) software and data were statistically evaluated with Microsoft Excel 2007.

Auxin transport assays in tobacco BY-2 cells, baker's yeast and Arabidopsis thaliana protoplasts

Auxin accumulation with 2-day-old BY-2 cells was measured as previously described14, 23. The 3H-IAA was added to give a final concentration of 2 nM. Accumulation results were expressed as pmols of particular auxin accumulated per 106 cells. The 0.5-ml aliquots of cell suspension were collected continuously and accumulation of label was terminated by rapid filtration under reduced pressure on 22-mm-diameter cellulose filters. The cell cakes and filters were transferred to scintillation vials, extracted in 0.5 ml of 96% ethanol for 30 min, and afterwards 4 ml of scintillation solution (EcoLite Liquid Scintilation Fluid, MP Biomedicals) was added. Radioactivity was determined by liquid scintillation counter Packard Tri-Carb 2900TR (Packard-Canberra, Meridian). Yeast 3H-IAA loading was quantified with the unspecific 14C-benzoic acid as control assayed in parallel and performed as previously described24. Relative export is calculated from yeast-retained radioactivity as follows: ((radioactivity in the yeast at time t = 10 min) − (radioactivity in the yeast at time t = 0)) × (100%)/(radioactivity in the yeast at t = 0 min). Unspecific loading due to diffusion was eliminated by vector control subtraction. IAA export from Arabidopsis thaliana mesophyll protoplasts was analysed as described16.

HPLC metabolic profiling in tobacco BY-2 cells

Two-days-old BY-2 cells were prepared for the experiment by equilibration in uptake buffer as already described for accumulation assays14. Experiments were done in uptake buffer and under standard cultivation conditions. Cells were incubated with addition of 20 nM 3H-IAA for a period of 0 and 20 min. Cells and media (uptake buffer) were collected and frozen in liquid nitrogen (100 mg of fresh weight and 5 ml per sample). Extraction and purification of auxin metabolites in cells and media were performed as described25, 26. The metabolites were separated on HPLC consisting of autosampler and 235C diode array detector (Perkin Elmer), column Luna C18 (2), 150 × 4.6 mm, 3 µm (Phenomenex, Torrance, USA), mobile phase A: 40 mM CH3COONH4, (pH 4.0) and mobile phase B: CH3CN/CH3OH, 1/1, (v/v). Flow rate was 0.6 ml min−1 with linear gradient 30–50% B for 10 min, 50–100% B for 1 min, 100% B for 2 min, 10–30% B for 1 min. The column eluate was monitored on 235C DAD followed by Ramona 2000 flow-through radioactivity detector (Raytest GmbH) after online mixing with three volumes (1.8 ml min−1) of liquid scintillation cocktail (Flo-Scint III, Perkin Elmer). The radioactive metabolites were identified on the basis of comparison of their retention times with authentic standards. For the results presentation the total integrated area of chromatogram plots has been normalized based on the equalization of total accumulated radiolabel.

In silico and phylogenetic analysis

PILS genes were identified via the SMART-protein tool from EMBL (http://smart.embl-heidelberg.de/)27, 28. Phylogenetic tree of AtPILS was constructed with the DNA-man software

version 4.0. PILS topologies were defined by the online HMM-top tool (http://www.enzim.hu/hmmtop/)29 and visualized by the TMRPres2D software (http://biophysics.biol.uoa.gr/TMRPres2D/download.jsp)30. PILS orthologues were identified with the online tool Plaza (http://bioinformatics.psb.ugent.be/plaza/)31.

Free IAA and conjugate measurements in Arabidopsis thaliana

For the quantification of free IAA and its amino acid conjugates, approximately 10 mg of plant material was taken into analysis. The samples were processed as previously described32 and quantified by UHPLC-MS/MS.

Used primers and vectors

Genotyping primers: pils2-1 RP, CTGGAGAAACCTGACATCTCG; pils2-1 LP, GATTGAAGCCGGCTTAAATTC; pils2-2 RP, CTGGAGAAACCTGACATCTCG; pils2-2 LP, TACCATTGATCTGTCTTCGGG; pils5-1 RP, TTGAGACCCGTATCATTGGAG; pils5-1 LP, TGTCCTGATAAAACCTTTTCAGG; pils5-2 RP, TACTGCACCGAAAATGAAACC; pils5-2 LP, TTGTACTATTTGCACCGGCTC.

Insert primer (LBb) (combine with RP): GCGTGGACCGCTTGCTGCAACT.

RT–PCR primers used for insertion lines: PILS2 Fw, GCGATCATTATCGGATCAGT; PILS2 Rev, TTGCATACCTTGGACAGTAGTC; PILS5 Fw, TGTTGAAGCCCGTAATTCCATGAAC; PILS5 Rev, TTCATTGCGGACCCTTTAATCAGC.

qPCR primers: PILS1 Fw, CGGTAACACAGCTCCACTTC; PILS1 Rev, GCAACAAGTAACGCACAACC; PILS2 Fw, GTGATGCTTGTACTTGGTGGTATG; PILS2 Rev, AACTTGAACATTGGATCTGCTGAG; PILS3 Fw, AGGCGACCATGCAAGTGTTG; PILS3 Rev, GTGGTACAGCTAGATGACAGTGAG; PILS4 Fw, TGTCATAACTAAGCCTCCTTCAC; PILS4 Rev, CTCGCAACTCTCAGAATCTCC; PILS5 Fw, CTTGGAATAGTCTGTGTTCGGTAC; PILS5 Rev, GCACTGAGCATTCGTCTTGAG; PILS6 Fw, GCCTACATCAGTGCTCTCAG; PILS6 Rev, GCACTGAGCATTCGTCTTGAG; PILS7 Fw, TCCTCCAGACCCTCTCTTTCG; PILS7 Rev, ACAAGAAGATGACCGAGCACTC; EiF4a Fw, CTGGAGGTTTTGAGGCTGGTAT; EiF4a Rev, CCAAGGGTGAAAGCAAGAAGA.

Cloning primers: gDNA/cDNA: PILS1_Fw, GGGGACAAGTTTGTACAAAAAAGCAGGCTCGATGAGGATGAGGCTTTTGGATC; PILS1_Rev, GGGGACCACTTTGTACAAGAAAGCTGGGTC(TCA)GGCTACGAGCCACATGAAGAATG; PILS2_Fw, GGGGACAAGTTTGTACAAAAAAGCAGGCTCGATGTCAGGTTTCTCCAGTGGAA; PILS2_Rev, GGGGACCACTTTGTACAAGAAAGCTGGGTC(TCA)TTGCATACCTTGGACAGTAGTCTC; PILS3_Fw,

GGGGACAAGTTTGTACAAAAAAGCAGGCTCGATGGTGAAGCTTTTGGAGCTGTTC; PILS3_Rev, GGGGACCACTTTGTACAAGAAAGCTGGGTC(TCA)AGCTACAAGCCACATGAAGAATG; PILS4_Fw, GGGGACAAGTTTGTACAAAAAAGCAGGCTCGATGAAGCTTTTGGAGTTGTTCA; PILS4_Rev, GGGGACCACTTTGTACAAGAAAGCTGGGTC(TCA)TGTCACAAGCCACATGAAGAATG; PILS5_Fw, GGGGACAAGTTTGTACAAAAAAGCAGGCTCGATGGGATTCTGGTCGTTGTTGGA; PILS5_Rev, GGGGACCACTTTGTACAAGAAAGCTGGGTC(TCA)GACTAACAAGTGAAGGAAGATGG; PILS6_Fw, GGGGACAAGTTTGTACAAAAAAGCAGGCTCGATGATTGCTCGGATCCTTGCCG; PILS6_Rev, GGGGACCACTTTGTACAAGAAAGCTGGGTC(TCA)GAAGAGTATGTTAATGTAGAGTAC; PILS7_Fw, GGGGACAAGTTTGTACAAAAAAGCAGGCTCGATGGGTTTCTTAGAGTTGTTGGA; PILS7_Rev, GGGGACCACTTTGTACAAGAAAGCTGGGTC(TCA)GGAGAGGATGGAGAGGAAGATGG.

Promoter: PILS2_Fw, GGGGACAACTTTGTATAGAAAAGTTGCGAACTCCATTGTTAACAGTAATAGC; PILS2_Rev, GGGGACTGCTTTTTTGTACAAACTTGCCTCGATCTCACTATGTAAAGCTCG; PILS5_Fw, GGGGACAACTTTGTATAGAAAAGTTGCGCAATATACGTGACGTGGTCCACT; PILS5_Rev, GGGGACTGCTTTTTTGTACAAACTTGCCTTTTTATGTGGTTCTTTAGAC.

Destination vectors: pPILS::GFP/GUS: pKGWFS7, p35S::PILS::GFP: pH7FWG2,0, p35S::GFP::PILS: pH7WGF2,0, p35S::PILS::RFP: pK7RWG2,0, p35S::RFP::PILS: pK7WGR2,0 and p35S::PILS_D: pH7WG2D,1 (ref. 33), and pPILS::PILS::GFP: pK7m34GW,0 (ref. 34).

Oestradiol-inducible PILS: pMDC7_B(pUBQ)35 (p35S promoter was exchanged by the pUBQ10 promoter).

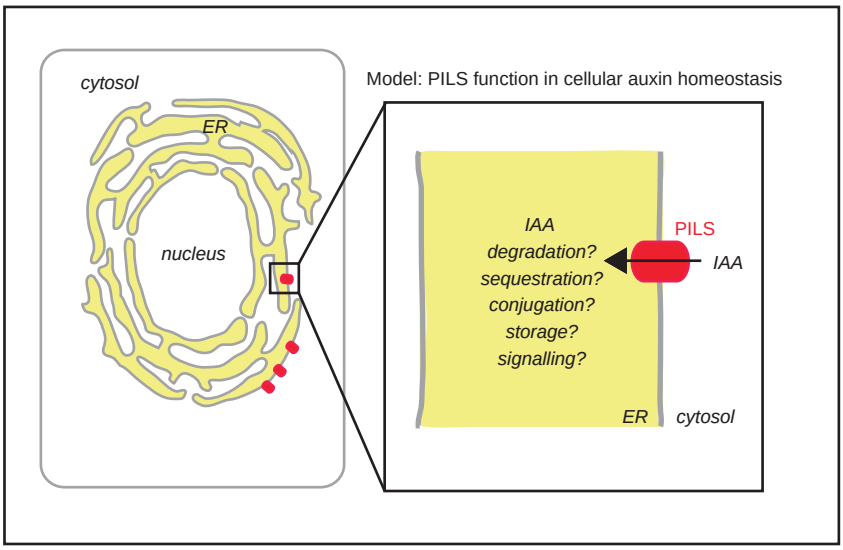

Supplemental Figure 1 Model on cellular PILS function.

PILS proteins localize to the endoplasmic reticulum (ER) and regulate cellular auxin accumulation, presumably by regulating auxin transport from the cytosol into the ER lumen. PILS function increases auxin conjugation-based inactivation of auxin and negatively regulates nuclear auxin signaling. We assume that both auxin sequestration into the ER and auxin conjugation might affect the availability of auxin for nuclear signalling. While our data may support a potential auxin conjugation in the ER, it remains to be seen whether known or yet to be discovered auxin amide conjugate synthetases function in the ER. To our knowledge, potential candidates of the GRETCHEN HAGEN (GH3) IAA amido synthetase family have not been localized in *Arabidopsis*, but in silico analysis of GH3 sequences do not suggest their residence in the ER[36]. In *Physcomitrella*, cytoplasmic localization was suggested for GH3-1 tagged with GFP[37]. Nevertheless, auxin metabolism is likely to be compartmentalized in the ER. Most known auxin conjugate hydrolyses, such as IAA-LEUCINE RESTISTANT1 LIKE (ILL) proteins, contain ER retention motifs[38,39], but their localization remains to be experimentally proven. Moreover, isoforms of YUCCA4 catalyzes auxin biosynthesis at the outer surface of the ER[40], possibly providing substrate for the auxin transport into the ER. Notably, also the auxin receptor AUXIN BINDING PROTEIN1 (ABP1) mainly resides in the lumen of the ER[41,42]. These results strongly suggest that auxin compartmentalization is important for plant development, but the unifying mechanism remains to be discovered.

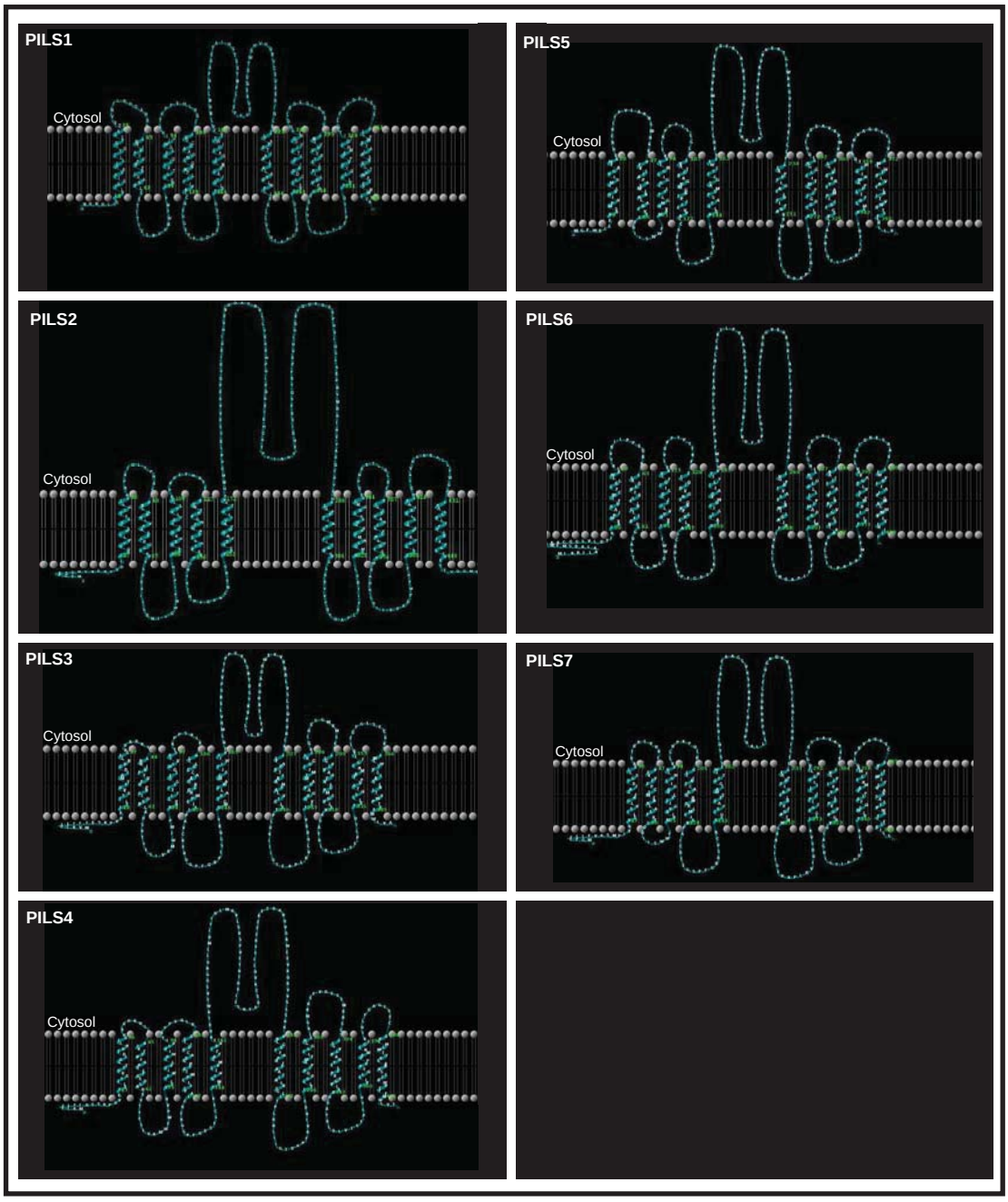

Supplemental Figure 2 PILS protein topologies.

In silico predicted transmembrane domain organization of PILS1-7 proteins.

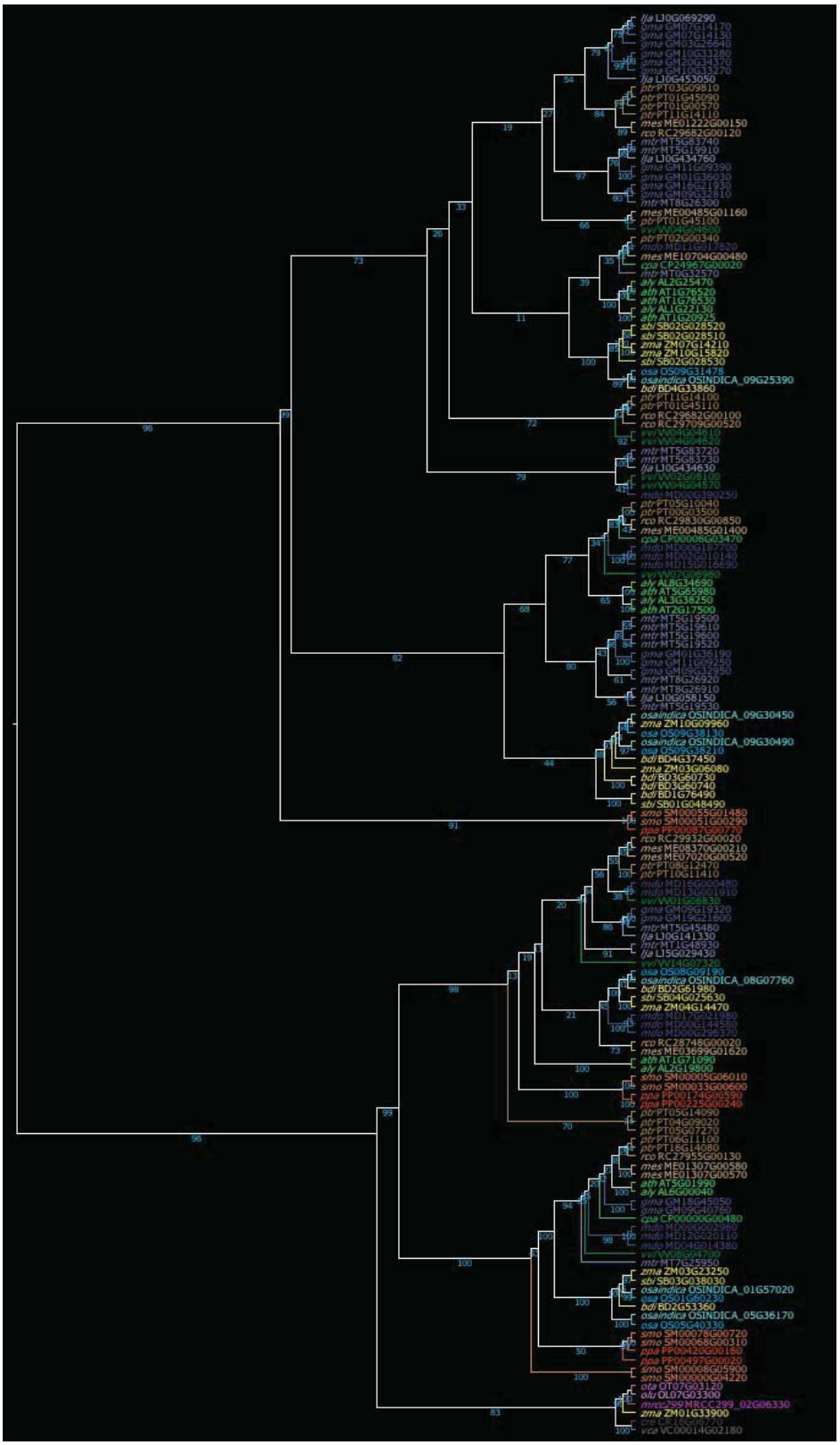

http://bioinformatics.psb.ugent.be/plaza/gene_families/explore_trees/HOM000497

Supplemental Figure 3 Phylogenetic tree of the PILS orthologues.

PILS orthologues in several plant species are identified and represented in a

phylogenetic tree using the Plaza2.0 online platform (*http://bioinformatics.psb.ugent.be/plaza/*[31,43]). Bootstrap values are given as percentages on the nodes.

Taxonomy abbreviations: *aly: Arabidopsis lyrata (light green) ; ath: Arabidopsis thaliana (light green); cpa: Carica papaya (green); gma: Glycine max (dark purple); lja: Lotus japonicas (light purple); mes: Manihot esculenta (light brown); mtr: Medicago truncatula (purple); osa: Oryza sativa (blue) spp. Japonica; osaindica: Oryza sativa spp. Indica (dark blue); ppa: Physcomitrella patens (red); ptr: Populus trichocarpa (dark brown); rco: Ricinus communis; sbi: Sorghum bicolor (yellow); vvi: Vitis vinifera (dark green); zma: Zea mays (yellow); mdo: Malus domestica; cre: Chlamidomonas reinhardtii (dark gray); mrcc299: Micromonas sp. RCC299 (dark bordeaux); ota: Ostreococcus tauri (bordeaux); smo: Selaginella moellendorfii (orange); vca: Volvox carteri (light gray); olu: Ostreococcus lucimarinus (light bordeaux); bdi: Brachypodium distachyon (dark yellow)*

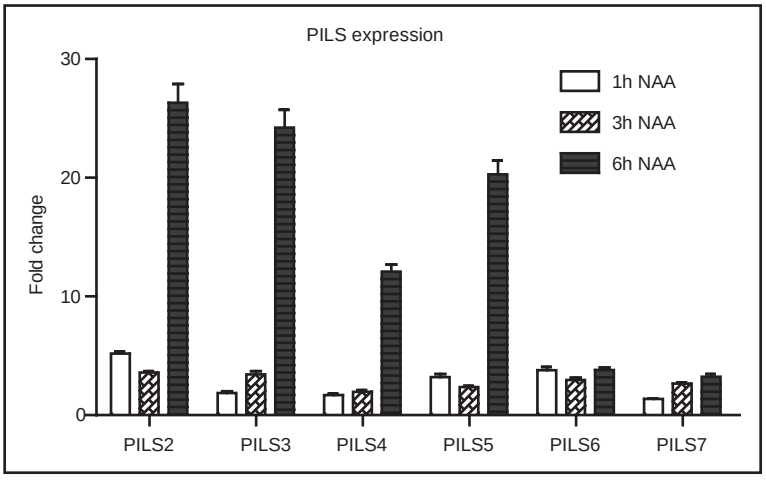

Supplemental Figure 4 qPCR analysis of auxin induced PILS expression.

The effect of 10µM NAA treatment for 1, 3 and 6 h on PILS expression levels was analyzed via quantitative RT-PCR. Graph depicts fold change in PILS expression upon auxin treatment compared to PILS expression levels in untreated seedlings. (n=3 repetitions) Error bars depict s.e.m..

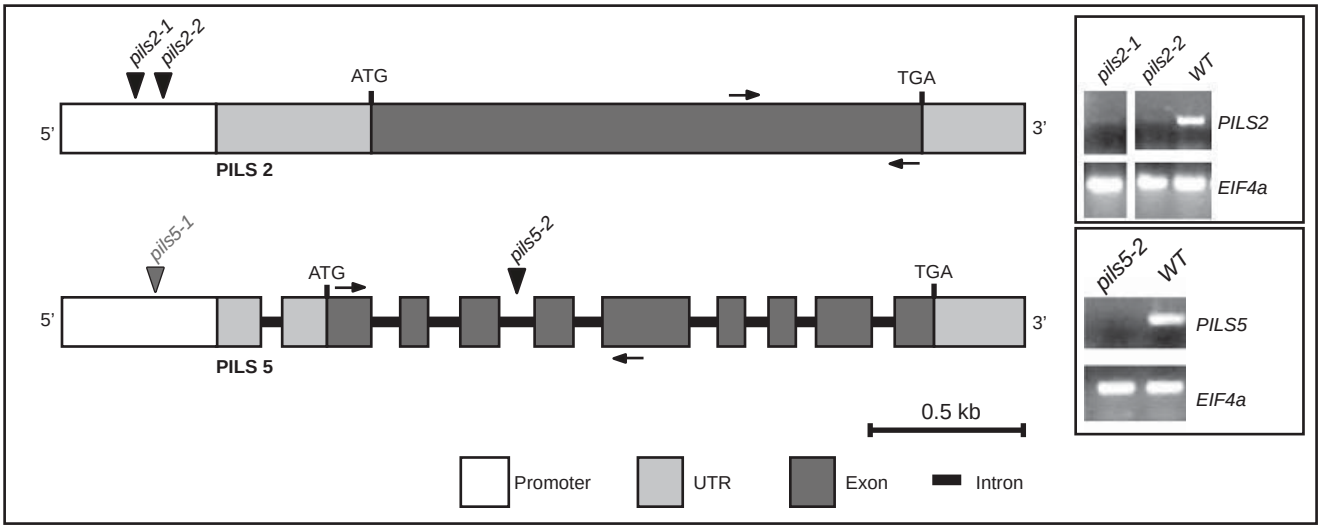

Supplemental Figure 5 PILS2 and PILS5 gene structure.

The PILS2 and PILS5 genes contain 1 and 9 exons, respectively. The analyzed T-DNA insertions are depicted in the figure (arrow heads). The PILS2 and PILS5 expression levels in the respective insertion lines were analysed by RT-PCR (given in the right panels). Arrows depict the annealing position of the used RT-PCR primers. *pils2-1* and *pils2-2* showed a strong reduction in transcription level. We did not detect PILS5 mRNA in the *pils5-2,* suggesting a full knock-out mutant. In contrast, PILS5 mRNA levels in the *pils5-1* mutant where similar to wild type (not shown). Scale bar, 500bp.

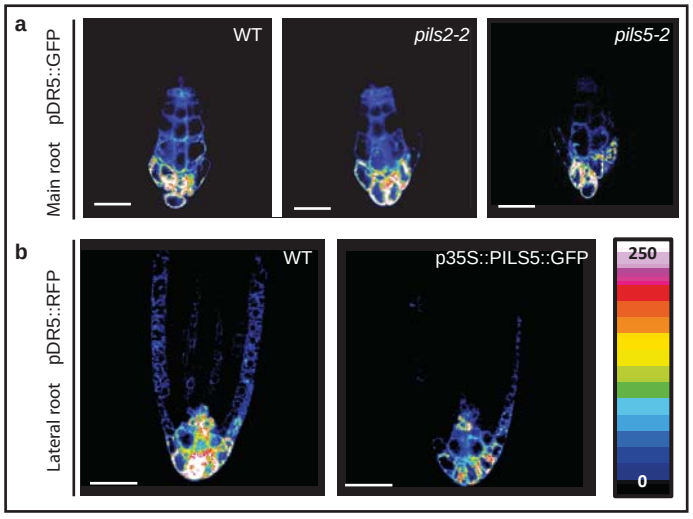

Supplemental Figure 6 Nuclear auxin signaling in pils loss- and gain-of-function mutants.

a,b Analysis of the auxin reporter *pDR5rev::GFP* (a) or *pDR5rev::mRFP1er* (b) expression reveals no change in auxin signaling in the main root of *pils2-2* and *pils5-2* single mutants compared to wild type (WT) (a). Lateral roots of seedlings overexpressing PILS5 display decreased auxin signaling compared to WT. Representative pictures are shown and a color-coded heat map (black to white) was used to visualize (low to high) pDR5rev::mRFP1er and pDR5rev::GFP signal intensity.

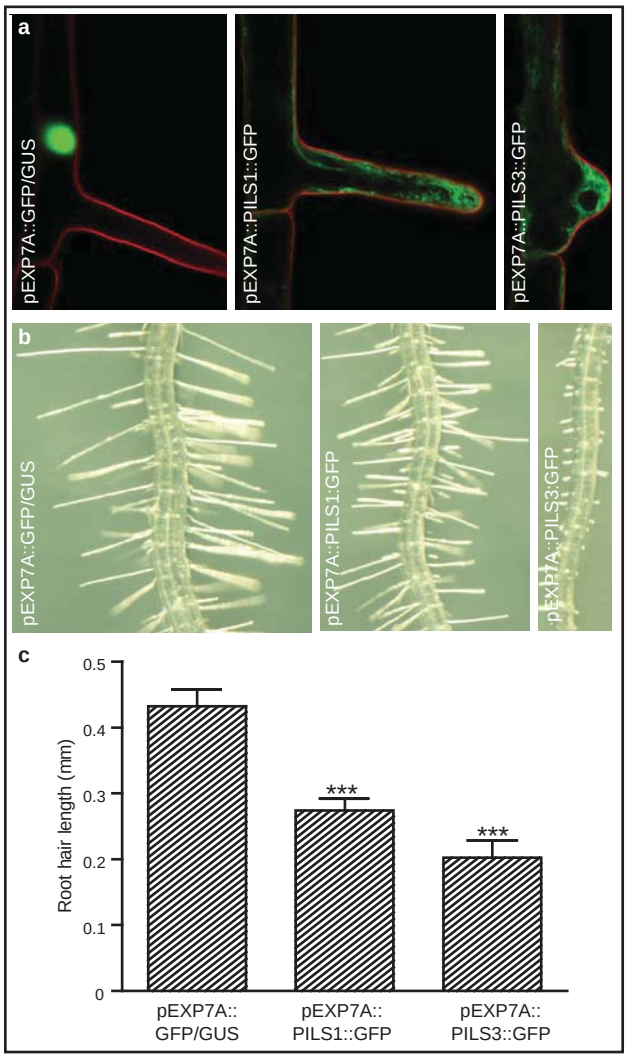

Supplemental Figure 7: Root hair cell-specific PILS activity represses root hair growth.

a, NLS-GFP::GUS (left), PILS1::GFP (middle) and PILS3::GFP (right) in root hairs (green). Propidium iodide staining in red. **b-c,** Root hair specific pEXP7A::PILS1::GFP and pEXP7A::PILS3::GFP expression represses root hair growth. **c,** Graph depicts the root hair length of seedlings expressing pEXP7A::GFP/GUS or pEXP7A::PILS1/3::GFP in the root hair cells (n=20 seedlings with 400 counted root hairs in total). Error bars represent s.e.m..

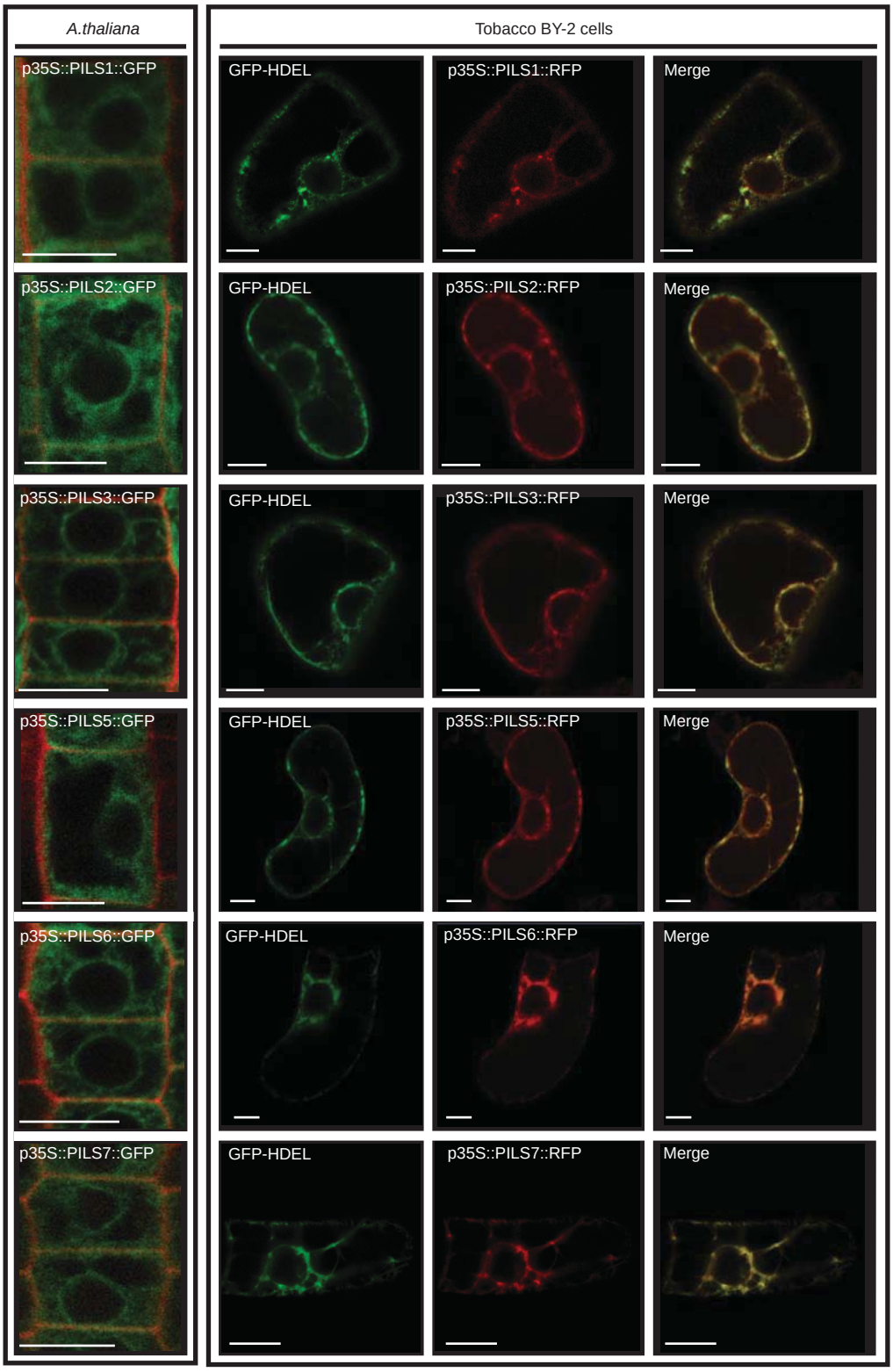

Supplemental Figure 8 PILS intracellular localization.

PILS(1-3)::GFP and PILS(5-7)::GFP fusion proteins reveal intracellular PILS localization to the ER as shown by live cell imaging of p35S::PILS::GFP in

A.thaliana root cells (left panel). Propidium iodide stained cell walls in red. Transient co-expression of PILS(1-3)::RFP and PILS(5-7)::RFP protein fusions and the ER-marker GFP-HDEL in tobacco BY-2 cells shows complete colocalization (right panel). PILS4::GFP/RFP did not show detectable fluorescence (not shown). Scale bar, 10μm.

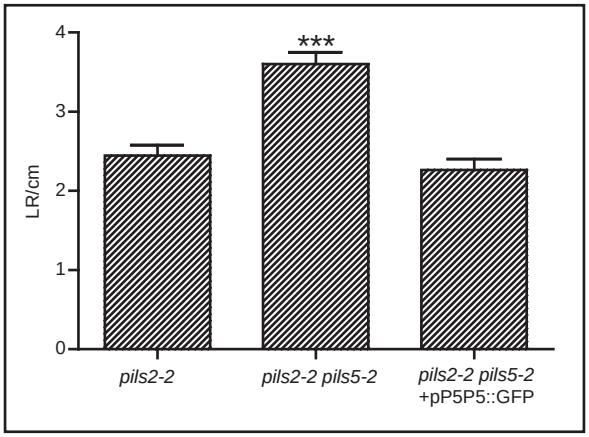

Supplemental Figure 9 *pils2-2 pils5-2* mutant complementation.

PILS5 expression under its endogenous promoter complements the enhanced lateral root density phenotype of the *pils2-2 pils5-2* loss-of-function mutant (n=40 seedlings). Error bars represent s.e.m. Student t-test P-values: *P< 0.05, **P<0.001 ***P<0.0001.

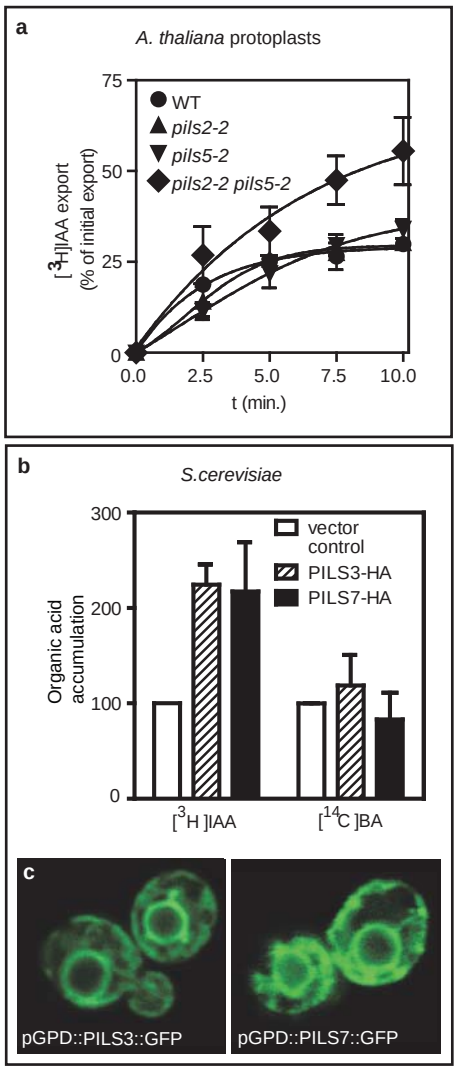

Supplemental Figure 10 PILS-dependent auxin accumulation in plant and non-plant cells

a, Arabidopsis protoplasts of *pils2-2 pils5-2* mutant leaves show higher ^{3}H-IAA export compared to protoplasts from wild type (WT) leaves (n=3 repetitions). Error bars represent s.e.m. **b,** Auxin accumulation assay in the *Saccharomyces cerevisiae* yeast cells. Cells transformed with pGPD::PILS3::HA or pGPD::PILS7::HA display higher auxin but not benzoic acid accumulation compared to cells transformed with an empty vector (n=3 repetitions). **c,** PILS3::GFP and PILS7::GFP localization in *Saccharomyces cerevisiae*. Error bars represent s.e.m..

References for supplemental figures:

[36] Ludwig-Müller, J., Auxin conjugates: their role for plant development and in the evolution of land plants. *J. Exp. Bot* **62**, 1757-1773 (2011).

[37] Ludwig-Muller, J., Julke, S., Bierfreund, N.M., Decker, E.L., & Reski, R., Moss (Physcomitrella patens) GH3 proteins act in auxin homeostasis. *New Phytol* **181**, 323-338 (2009).

[38] LeClere, S., Tellez, R., Rampey, R.A., Matsuda, S.P., & Bartel, B., Characterization of a family of IAA-amino acid conjugate hydrolases from Arabidopsis. *J Biol Chem* **277**, 20446-20452 (2002).

[39] Campanella, J.J., Larko, D., & Smalley, J., A molecular phylogenomic analysis of the ILR1-like family of IAA amidohydrolase genes. *Comp Funct Genomics* **4**, 584-600 (2003).

[40] Kriechbaumer, V., Wang, P., Hawes, C., & Abell, B.M., Alternative splicing of the auxin biosynthesis gene YUCCA4 determines its subcellular compartmentation, *Plant J*. doi: 10.1111/j.1365-313X.2011.04866.x (2012)

[41] Jones, A.M. & Herman, E.M., KDEL-Containing Auxin-Binding Protein Is Secreted to the Plasma Membrane and Cell Wall. *Plant Physiol* **101**, 595-606 (1993).

[42] Henderson, J., Bauly, JM., Ashford DA, Oliver SC, Hawes CR *et al.*, Retention of maize auxin-binding protein in the endoplasmic reticulum: quantifying escape and the role of auxin. *planta* **202**, 313-323 (1997).

[43] Zmasek, CM., Eddy, SR., ATV: display and manipulation of annotated phylogenetic trees. *Bioinformatics.* **17**, 383-384 (2001).